Incorporating Power Electronic Converters Reliability Into Modern Power System Reliability Analysis

Saeed Peyghami, *Member, IEEE*, Frede Blaabjerg, *Fellow, IEEE*, and Peter Palensky, *Senior Member, IEEE*

***Abstract*— This article aims to incorporate the reliability model of power electronic converters into power system reliability analysis. The converter reliability has widely been explored in device- and converter-levels according to physics of failure analysis. However, optimal decision-making for design, planning, operation, and maintenance of power electronic converters require system-level reliability modeling of power electronic-based power systems. Therefore, this article proposes a procedure to evaluate the reliability of power electronic-based power systems from the device-level up to the system-level. Furthermore, the impact of converter failure rates including random chance and wear-out failures on power system performance in different applications such as wind turbine and electronic transmission lines is illustrated. Moreover, because of a high calculation burden raised by the physics of failure analysis for large-scale power electronic systems, this article explores the required accuracy for reliability modeling of converters in different applications. Numerical case studies are provided employing modified versions of the Roy Billinton Test System (RBTS). The analysis shows that the converter failures may affect the overall system performance depending on its application. Therefore, an accurate converter reliability model is, in some cases, required for reliability assessment and management in modern power systems.**

***Index Terms*— Adequacy, converter reliability, high-voltage direct current (HVDC) reliability, reliability, wear-out failure, wind farm (WF) reliability.**

I. Introduction

ELECTRIC power system modernization is essential for reliable and secure power delivery with a low-to-zero carbon footprint. It requires deploying new technologies and infrastructure as well as deregulating the electricity sector. Some established technologies have a considerable role in power systems modernization including renewable energy resources, storages, electronic transmission and distribution systems, and e-mobility. Notably, power electronics (PE) plays an underpinning role in the energy conversion process of the aforementioned technologies [1]. Particularly, moving toward one hundred percent renewable energies has intensified the importance of PE in the future power systems. However, power converters are one of the frequent source of failures in many applications [2]–[4], hence introducing high downtime and maintenance costs [2]–[11] is imperative. Moreover, according to field data and industrial experiences, the power converters are exposed to aging and wear-out failures depending on the operating conditions [3]–[5], [12], [13].

A power converter is made up of various subsystems including power modules, capacitors, gate drivers, control units, and cooling system. Electrolytic capacitors and power modules are the two most fragile components which are also prone to wear-out failure. The reliability of these components depends on different factors such as device mechanical strength, applied electrical load, climate conditions, and control and switching schemes. These factors cause degradation of component materials during long-term operation of the converter, finally triggering the potential failure mechanisms. The physics of failure-based stress–strength analysis (SSA) for different failure mechanisms can be used for component reliability prediction and enhancement from a wear-out standpoint.

The SSA requires electrothermal modeling in three hierarchical levels including device-level, converter-level, and system-level [14]. The system-level modeling identifies the loading of the converter according to its application in the power system. For instance, the loading of parallel-connected converters depends on power-sharing strategies. Moreover, the converter-level studies include electrical domain modeling and simulations in order to find out the stress of each component under applied control and switching strategies. Finally, the device-level analysis requires electrothermal modeling of devices for obtaining key thermal variables, such as hot-spot temperature, which are enabling failure mechanisms under a given mission profile. As a result, the SSA analysis comprises very fast dynamics in the range of switching frequency at the device-level to the slow dynamics in the range of hourly load changes at the system-level. Therefore, the wear-out failure prediction over an annual mission profile is a time-consuming process. In the system-level analysis, it will introduce a very high calculation burden especially in large-scale power systems.

Manuscript received November 13, 2019; revised January 13, 2020; accepted January 13, 2020. Date of publication January 17, 2020; date of current version April 1, 2021. This work was supported by the Reliable Power Electronic-Based Power System (REPEPS) Project at the Department of Energy Technology, Aalborg University, as a part of the Villum Investigator Program funded by the Villum Foundation. Recommended for publication by Associate Editor Philip T. Krein. *(Corresponding author: Saeed Peyghami.)*

Saeed Peyghami and Frede Blaabjerg are with the Department of Energy Technology, Aalborg University, 9220 Aalborg, Denmark (e-mail: sap@et.aau.dk, fbl@at.aau.dk).

Peter Palensky is with Faculty of Electrical Engineering, Mathematics and Computer Science (EEMCS), Delft University of Technology, 2600 AA Delft, The Netherlands (e-mail: p.palensky@tudelft.nl).

Color versions of one or more of the figures in this article are available online at https://ieeexplore.ieee.org.

Digital Object Identifier 10.1109/JESTPE.2020.2967216

So far, the SSA has been employed in device-level for lifetime modeling and extension in capacitors and semiconductor devices [12], [15]–[19]. In the converter-level, the SSA is used for converter lifetime extension by active thermal management approaches such as appropriate modulation strategies [20]–[22], adaptive switching frequency [23], and active/reactive power control [24]–[26]. The converter topologies and photovoltaic array characteristics are other factors affecting the converter lifetime [22], [27], [28]. Furthermore, the capacitors lifetime expansion is explored in [27] and [28] by interleaving the converters. Moreover, the system-level reliability enhancement in multiconverter systems is performed by appropriately modifying the converters loading and shifting the device damages from high-stressed converter to the low-stressed one [14], [29].

The aforementioned reliability analyses in [11] and [14]–[29] are limited to the converter lifetime prediction and enhancement even at the system-level studies. However, optimal decision-making in design, planning, operation, and maintenance of the converters in the power systems requires analyzing their impacts on power system reliability. This requires bridging the power electronic reliability concepts and the power system reliability assessment approaches.

The power system reliability is defined as a measure of its ability to cope with customer demands [30]. Technically, this ability is measured by adequacy indices such as loss of load expectation (LOLE) and expected energy not supplied (EENS) [30]. Besides, the conventional power systems reliability analysis [30], the reliability of power electronic-based power systems such as wind farms (WFs) and high-voltage direct current (HVDC) transmission systems have been widely studied, e.g., in [30]–[39] and [36], [40], [41]. Moreover, the reliability of microgrid systems considering the impact of power electronic converters has been explored in [31]. In the state-of-the-art research [30]–[39], [36], [40], [41], the failure rate of converters in power system analysis is obtained from the historical data of similar cases. Moreover, the wear-out failure of converters has not been taken into account in the power system reliability assessment. In practice, the wear-out of converter components may happen earlier than the expected lifetime [12]. Therefore, not only the failure rate of the converter during operation will be increased, but also its end-of-life will be limited. Hence, the converter components aging will affect the overall system reliability and risk, consequently inducing higher downtime and maintenance costs especially in the large-scale power electronic-based power systems.

In order to avoid these issues, appropriate strategies must be adopted for optimal decision-making in planning, operation, and maintenance of modern power electronic-based systems. This requires system-level reliability analysis by incorporating the converter reliability modeling in power system reliability assessment. This procedure is very time-consuming, and in practice, for large-scale power systems is almost impossible. This is due to the fact that the electrothermal modeling based on SSA requires time-domain analysis with the time frame of interest from microsecond associated with the converter switching frequency up to the hourly load variations. Therefore, system-level reliability modeling in power electronic-based systems need simplified electrothermal modeling techniques in different time frames.

According to the aforementioned issues posed by the proliferation of converters in power systems, this article aims to address the following challenges.

1) Since any decision-making regarding converters operation, planning, and maintenance must be performed at the system-level, hence, the system-level reliability modeling in power electronic-based systems is of high importance. This article aims at bridging the converter reliability models and power system reliability concepts for evaluating the reliability of power electronic-based power systems.
2) Due to the increasing use of converters in power systems, their failure rates associated with the random chance and wear-out failures may affect the overall performance of power systems. This article will illustrate the impact of converter failures and aging on the power system reliability.
3) Due to the complexity of the reliability modeling in converters based on SSA, the simplified approaches should be introduced for system-level analysis. This article presents the required accuracy of converter reliability modeling for power system analysis in different applications.
4) The converter failure rate will be increased due to the aging of components. Thereby, they must be replaced according to a suitable maintenance strategy. The impact of run-to-fail and age replacement policies on the power system reliability is presented in this article.

In order to achieve the above-mentioned goals, Section II presents the concept of reliability in PE and power systems and their correlations. Section III represents the reliability modeling in power electronic converters. The reliability evaluation in power systems and incorporation of converter reliability in power system analysis are presented in Section IV. Numerical analyses are provided in Section V. Finally, the outcomes are discussed and summarized in Sections VI and VII.

II. Concept of Reliability

Reliability is defined as the ability of a system or an item to function under desired conditions within a specific period of time [42], [43]. According to this definition, the system/item performance must be retained within a specified interval at a target time period. Depending on a system, the reliability measures may be different. For instance, in a mission-based system, such as a spacecraft, the reliability is defined as the probability of survival during the target mission period. Thus, the first time to failure with a desired probability must be longer than the target mission period. Furthermore, in a maintainable/repairable system/item with the possibility of maintenance, the performance is measured by the availability as its reliability indicator. In these systems/items, it is important to have them in the operation state (being available) at any instance regardless of any failure occurrence before that time [43]. This means that the system can be maintained whenever it fails and hence the only issues are the failure frequency and downtime.

A power system as a complex combination of a large number of subsystems and components should operate all the time for a long period of time. According to this expression, the power system performance, which is to supply its demand, must be guaranteed at all times. The short-term performance of power systems is associated with the operation phase, which is defined as its ability to withstand any contingencies and outages. This ability is defined as a security that is related to the stability of power systems [44]. Moreover, long-term performance of the power system is associated with its ability to supply the load considering the uncertainty in generation availability and load level. This requires having adequate generation, transmission, and distribution facilities. This ability is known as power system adequacy, which is a measure used for design and planning (facility and/or operational planning) [44]. As a result, the power system reliability is defined as its ability to supply the demand in a short term by responding to the contingencies and in a long term by installing and employing adequate facilities. According to this definition, the facilities must have an acceptable level of availability to guarantee system performance.

One of the important measures of power system performance is loss of load/energy. The loss of load can be measured by different indices such as loss of load probability (LOLP), LOLE, and EENS [30], [43], [45], [46]. As a result, the power system reliability can be measured by loss of load indices. For instance, a reliable power system may have LOLE from 4 to 8 h per year [46]. A system with a higher value of LOLE is known as an unreliable system. Based on this definition, the failure of one or more components might or might not affect the power system reliability. In order to achieve a reliable power system, the components and subsystems must be maintained or replaced to improve their availability whenever it is required. Therefore, the availability of components is one of the main reliability indicators in power systems.

In modern power systems, power electronic converters are one of the vulnerable components, which are also prone to wear-out failures [3]–[5], [12], [13]. Aging of converters will affect the overall system reliability since the higher failure rate will introduce lower availability. Therefore, reliability modeling in power electronic converters as an underpinning technology of future power grids [1] is of paramount importance. The wear-out-related reliability of converters depends on its aging-prone components such as capacitors and power modules. The reliability of these components is defined as the probability of survival within a target operating time. The failure rate of components can be thus found by failure probability function $F(t)$. This failure probability function depends on the operating conditions and lifetime model of devices, where the lifetime of power modules is related to the number of cycles to failure N_{f} and the lifetime of capacitors is associated with the time to failure L_{o} [47].

Therefore, the reliability of power electronics-based power systems can be modeled in three levels as shown in Fig. 1 [14]. In the component level, the lifetime model of the component is employed to predict their failure rate by wear-out failure modeling under given operating and climate conditions. Then, the failure rate of components is used to model the converter reliability and failure rate based on the functionality of different components in the subsystem-level. Afterward, the converters availability is predicted according to the maintenance strategies. The availability of converters is incorporated into the power system reliability analysis to predict the system reliability indices such as LOLE and EENS. Moreover, according to the overall system reliability, proper maintenance times can be scheduled to obtain a desired level of reliability. This procedure is comprehensively explained in the following sections for a power electronic-based power system. It is exemplified for a wind-based renewable energy generation system.

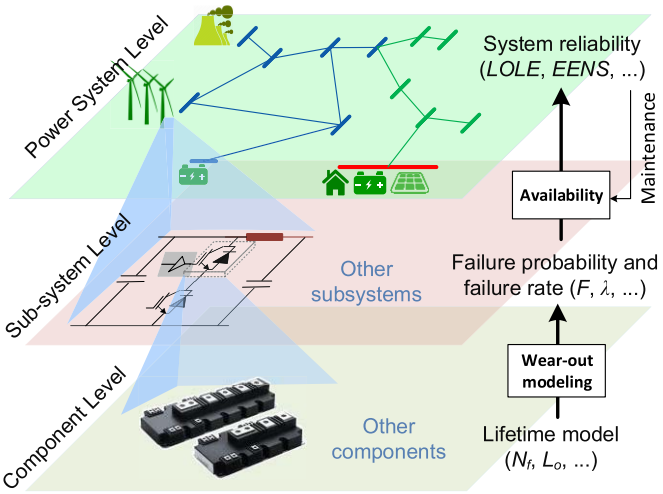

Fig. 1. Correlation between PE and power system reliability concepts.

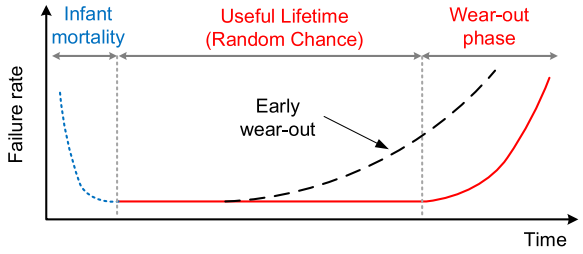

Fig. 2. Typical failure shape of an item known as bathtub curve.

III. Converter Reliability Modeling

The failure characteristics of a converter, like other systems, comprise three periods including infant mortality, useful lifetime, and wear-out phase as shown in Fig. 2 known as the bathtub curve. Usually, the infant mortality failures are related to the debugging and manufacturing processes. Hence, the converter will experience the random chance and wear-out failures within operation. The random chance failures usually have external sources such as overcurrent and overvoltage [47]. Therefore, they are considered as exponentially distributed failures within the useful lifetime in the bathtub curve [47]–[49]. The corresponding failure rate is usually predicted based on the historical reliability data and operational experiences. Moreover, the wear-out failure rate is associated with the aging and degradation of device materials over a long-term

operation and they are modeled by SSA over the aging-prone components.

Following field data, the power modules (i.e., semiconductor devices) and capacitors are the most fragile converter components. The lifetime model of the electrolytic capacitors is obtained by [50]

$$L_{\mathrm{o}} = L_n \cdot 2^{\frac{T_n - T_{\mathrm{o}}}{n_1}} \left(\frac{V_{\mathrm{o}}}{V_n}\right)^{-n_2} \tag{1}$$

where L_n is the nominal lifetime under nominal voltage V_n and upper category temperature T_n, and L_{o} is the capacitor lifetime under operating voltage V_{o} and temperature T_{o}. The exponents of n_1 and n_2 are obtained by lifetime testing [50]. Furthermore, the number of cycles to failure, N_{f} in semiconductor devices is calculated by using [51]

$$N_{\mathrm{f}} = A \cdot \Delta T_j^{\alpha} \cdot \exp\left(\frac{\beta}{T_j}\right) \cdot \left(\frac{t_{\mathrm{on}}}{1.5}\right)^{-0.3} \tag{2}$$

where ΔT and T are the junction temperature swing and its average value, and t_{on} denotes the rise time of temperature cycle. The constants of A, α, and β are curve-fitting constants obtained from aging tests [51]. Notably, the junction temperature depends on the thermal loss of device, its thermal impedance and ambient temperature. Moreover, the thermal loss comprises two terms of conduction loss and switching loss [52], where the conduction loss is associated with the device current, voltage, ON-state resistance. Furthermore, the switching loss depends on switching frequency and ON–OFF energy loss. In order to obtain the lifetime of the devices, the annual mission profile should be translated to thermal variables in (1) and (2), i.e., temperature, and voltage, through electrothermal analysis. This procedure is shown in Fig. 3(a). Therefore, the detailed electrical and thermal model of converter components must be employed which requires time-domain analysis.

Following Fig. 3(a), the reliability prediction procedure consists of two stages, where the first stage is in charge of electrothermal modeling, and the second stage is associated with reliability modeling. The first stage comprises two different domains of electrical and thermal domains, where the annual mission profile (which can be solar irradiance, wind speed, ambient temperature, and so on) is translated into the electrical variables, such as device voltage and current profile, and then thermal variables, such as junction and hotspot temperature. This process requires electrical modeling with the dynamics of switching frequency (several kilohertz to several ten kilohertz depending on the converter capacity) over the whole mission profile with different power levels. Moreover, the lifetime of power devices depends on the junction temperature swing which is affected by the variation in the converter loading power and the thermal impedance of the device. The thermal impedance is usually modeled by a higher-order (3–5 orders) transfer function as shown in Fig. 3(a). In order to translate the mission profile variation into the junction temperature swing, which remarkably affects the switch lifetime according to (2), a detail electrothermal mapping is required. The complexity and calculation burden will be induced by solving the differential equation of a thermal model for the long-term mission profile to obtain the temperature variations.

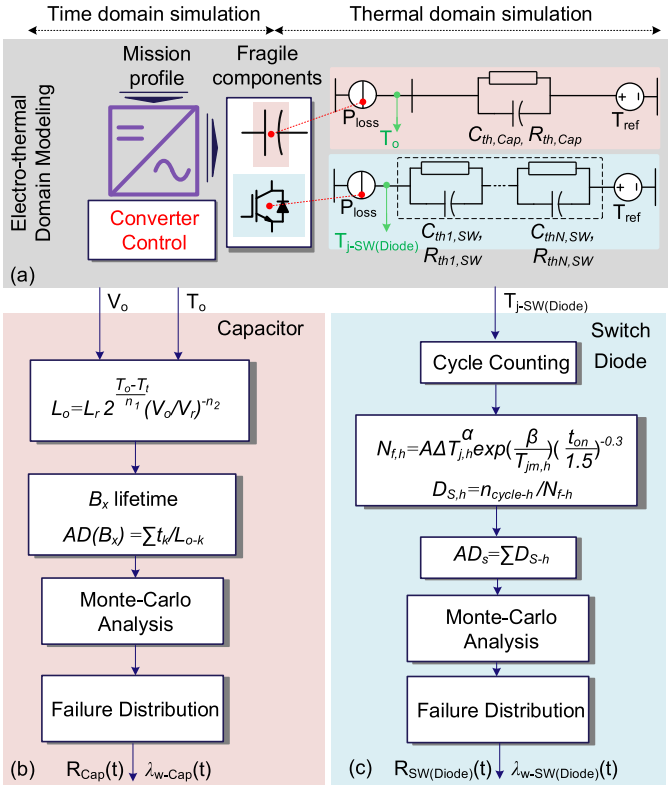

Fig. 3. Wear-out failure rate prediction in power converters. (a) Electrothermal mapping. (b) Wear-out failure rate of capacitors. (c) Wear-out failure rate of semiconductor devices.

After translating the mission profile into the thermal variables, the thermo-mechanical damage of the devices must be calculated to predict the converter lifetime. Accumulated damage of the capacitors ($\mathrm{AD_{Cap}}$) under a given mission profile is obtained as follows:

$$\mathrm{AD_{Cap}} = \sum_k \frac{t_k}{L_{\mathrm{o}-k}} \tag{3}$$

where t_k is the period that the capacitor operates under (V_{o}, T_{o}), and $L_{\mathrm{o}-k}$ is the corresponding lifetime obtained by (1).

Moreover, in order to obtain the accumulated damage of semiconductor devices ($\mathrm{AD_S}$), the junction temperature profile is classified into different classes, where the class h is defined as a set of variables (T_h, ΔT_h, $t_{\mathrm{on}-h}$, $n_{\mathrm{cycle}-h}$). The *ADs* is then obtained as follows:

$$\mathrm{AD}_S = \sum_h \frac{n_{\mathrm{cycle\text{-}h}}}{N_{\mathrm{f\text{-}h}}} \tag{4}$$

where $n_{\mathrm{cycle}-h}$ is the number of cycles in class h and $N_{\mathrm{f\text{-}h}}$ is the corresponding number of cycles. The device lifetime is equal to the reciprocal of the AD in (3) and (4). The obtained AD values for each devices are associated with the specific values of lifetime models in (1) and (2) as well as specific thermal models of devices. In practice, the lifetime models and device thermal characteristics have uncertainties with a certain range of variations. Therefore, the distribution of AD in terms of model and manufacturing uncertainties must be identified. The AD distribution function can be obtained by Monte Carlo simulations as shown in Fig. 3(b) and (c). Notably, employing

Monte Carlo simulations for reliability modeling will be also a time-consuming process. The reciprocal of the AD distribution function is known as the device unreliability function, $F(t)$. Once, the unreliability function is obtained, the wear-out failure rate of components can be calculated as follows:

$$\lambda_{w-X}(t) = \frac{1}{1-F(t)}\frac{d}{dt}F(t) \tag{5}$$

where d/dt is the differential operator and λ_{w-X} denotes as the wear-out failure of device X. Usually, the wear-out failure rate is modeled by a Weibull distribution function with a hazard function of $h(t)$ as follows:

$$h(t) = \lambda_{w-X}(t) = \beta\alpha^{-\beta}t^{\beta-1} \tag{6}$$

where α and β are the scale and shape factors of Weibull distribution. Finally, the device X failure rate λ_X is obtained by using

$$\lambda_X(t) = \lambda_{w-X}(t) + \lambda_{c-X} \tag{7}$$

where λ_{c-X} denotes the constant failure rate within a useful lifetime, which can be predicted based on historical failure data and operational experiences.

IV. Power System Reliability

Power system reliability, the so-called adequacy is a measure of its ability to meet the electric power and energy requirements of the customers within the acceptable technical limits considering the component outages [53]. The main measure employed in power system reliability assessment is the availability of its components. Availability is defined as the probability that an item is in operating state at any instant t given that it started to operate at instant zero. This section will present the general concept of components availability with time-constant and time-varying failure rates. Moreover, the reliability of power systems and their subsystems will be presented.

A. Concept of Availability

Generally, the failure rate of components is considered constant (see Fig. 2) owing to the fact that they are regularly maintained and the wear-out rarely happens. It is worth mentioning that a run-to-fail replacement strategy is employed for availability prediction in this article. For exponentially distributed systems, the availability can be obtained by using the Markov process (MP). Following the MP, system states can be represented as being in the operating state of "1" and being in down state "2" as shown in Fig. 4(a). The system availability, A according to the MP is the probability of being in state "1," which is obtained as follows [43]:

$$A = 1 - \text{FOR} = \frac{\mu}{\lambda+\mu} \tag{8}$$

where λ and μ are the failure and repair rates within the useful lifetime, respectively. Forced outage rate (FOR) is defined as the unavailability following (8).

For the systems with nonexponential failures, the MP cannot be utilized. In this case, the failure rate can be decoupled

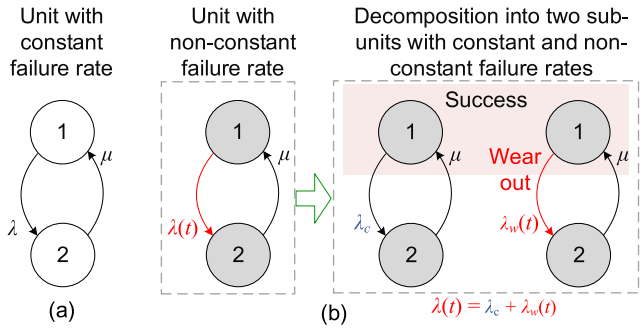

Fig. 4. State space modeling of a single unit. (a) Markov model used for analyzing a unit with constant failure rate λ. (b) General model with nonconstant failure rate $\lambda(t)$ which is decomposed into two subunits with time-constant failure rate λ_c and time-varying failure rate λ_w. The unit success will be achieved if and only if both subunits stay at operating state of "1."

into constant and time-varying terms. The cause of random chance failures in converter components such as capacitors and semiconductor devices are induced by abnormal operation and sudden over-stressing the components, whereas the wear-out failures are due to the long-term degradation of the component materials. Therefore, they have independent failure causes, and decoupling the failure rate into constant and time-varying terms is an appropriate assumption. As a result, a system with nonconstant failure rate shown in Fig. 4(b) can be converted into two subsystems with time-constant failure rate shown in Fig. 4(c) and time-varying term as shown in Fig. 4(d). According to Fig. 4(c) and (d), the system is available if and only if both subsystems are available. Therefore, the total availability $A_t(t)$ can be obtained as follows:

$$A_t(t) = A_c \cdot A_w(t) \tag{9}$$

where $A_c(t)$ is associated with the time-constant failure rate obtained by using (8). Moreover, the $A_w(t)$ is related to the time-varying failure rate with the cumulative distribution function (CDF) of $F_{12}(t)$. In order to obtain the time-varying availability, the semi-Markov process (SMP) can be employed [54], [55]. According to SMP, the probability of being in state j if the process starts at state i, ζ_{ij} can be obtained by using the following equation [54]:

$$\zeta_{ij}(t) = \delta_{ij}(1 - F_{ij}(t)) + \sum_{\substack{k=1 \\ k\neq i}}^{2} \int_0^t \frac{d}{d\tau}F_{ik}(\tau)\cdot\zeta_{kj}(\tau - t)d\tau \tag{10}$$

where δ_{ij} is

$$\delta_{ij} = \begin{cases} 1, & i = j \\ 0, & i \neq j. \end{cases} \tag{11}$$

Following Fig. 4(d), $F_{12}(t)$ is the failure CDF and $F_{21}(t)$ is the repair CDF with a constant repair rate of μ. According to (10), the availability of the subsystem with time-varying failure rate is equal to the probability of being in state "1" given that the process has been started to operate in state "1,"

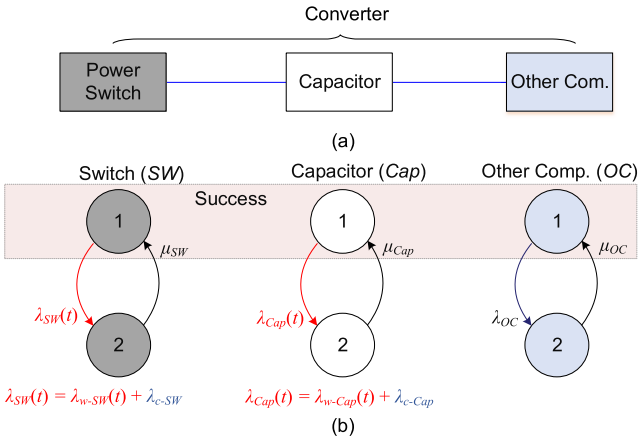

Fig. 5. Power converter availability model. (a) Availability block diagram. (b) Markov model. A converter success will be achieved if and only if all its components are in operating state "1."

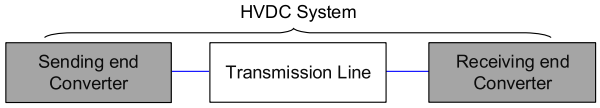

Fig. 6. HVDC system availability model.

hence

$$A_{to}(t) = \zeta_{11}(t). \tag{12}$$

B. Availability of Power Converters

The reliability of a converter can be modeled by its components' reliability as shown in Fig. 5(a). Since switches and capacitors are prone to wear-out failures [2], [19], their availability is modeled individually by using (9). The converter is available if and only if all the components are available as shown in Fig. 5(b). Hence, the overall converter availability is obtained by using the following equation:

$$A_{\text{con}}(t) = A_{\text{SW}}(t) \cdot A_{\text{Cap}}(t) \cdot A_{\text{OC}} \tag{13}$$

where $A_{\text{con}}(t)$, $A_{\text{SW}}(t)$, $A_{\text{Cap}}(t)$ and A_{OC} are the instantaneous availability of power switch (SW), capacitor (Cap) and other components (OC). $A_{\text{SW}}(t)$ and $A_{\text{Cap}}(t)$ are predicted by SMP using (9) and A_{OC} is predicted by MP using (8).

C. Availability of HVDC System

The HVDC system contains a sending end converter, a receiving end converter, and a dc transmission line. The HVDC system reliability can be modeled as a series network of these components as shown in Fig. 6. Hence, the availability of the HVDC system, $A_{\text{HVDC}}(t)$ is calculated as follows:

$$A_{\text{HVDC}}(t) = A_{\text{con,s}}(t) \cdot A_{\text{con},r}(t) \cdot A_{\text{DC}} \tag{14}$$

where $A_{\text{con,s}}(t)$ and $A_{\text{con,r}}(t)$ are the availability of the sending and receiving end HVDC converters (HCs) obtained by using (13), and A_{dc} is the availability of the dc line obtained by using (8).

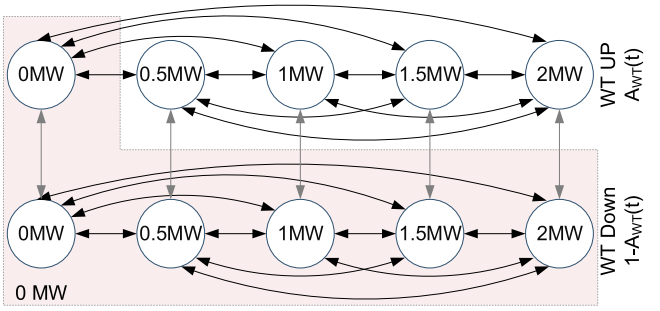

Fig. 7. 2-MW WT availability model—the highlighted states show zero generation due to either wind power unavailability or WT unavailability or both [32], [35], [37].

D. Availability of Wind Turbine

A wind turbine (WT) consists of different components such as blades, hub, generator, gear-box, converter, and control [36]. Similar to the HVDC system, the availability of the WT, $A_{\text{WT}}(t)$ can be obtained as follows:

$$A_{WT}(t) = A_{\text{con}}(t) \cdot A_{\text{OC}} \tag{15}$$

where $A_{\text{con}}(t)$ and A_{OC} denote the availability of WT converter (WTC) and other components. Due to the uncertainty in wind power, its availability should also be included in the WT availability. One approach to model the wind power availability is to discretize the output power of the WT into some states. For instance, in a 2-MW WT, its output power can be divided into 0, 0.5, 1, 1.5, and 2 MW as shown in Fig. 7. The probability of each state can be obtained by convolving the probability of wind power probability distribution with the WT characteristic curve [32], [35], [56]. Each state is available if the turbine is available. The availability of a 40-MW WF with 20 WTs can be obtained by combining the availability model of individual WT. Hence, the entire states will be 40, 39.5, 39,…, 0 MW. Therefore, like the conventional generation system [30], the capacity outage probability can be calculated for the WF. The detailed analysis has been discussed in [32] and [35]. According to Fig. 8, the wind power is available on the grid side if and only if the HVDC transmission line, i.e., WF converters (WFCs) and the dc line is available. Therefore, the total probability of each state must be convolved with the availability of WF HVDC line.

E. Reliability of WF

The performance of a WF can be measured by its availability [57]–[59]. Two kinds of availability measures can be defined for WFs including time-based availability A_{time} [57] and production-based availability A_{prod} [58]. The annual time-based availability is obtained by

$$A_{\text{time}} = 8760\left(1 - \frac{\text{Unavailable time}}{\text{Available time} + \text{Unavailable time}}\right)[h/y]. \tag{16}$$

Time-based unavailability is the complementary of the time-based availability. Moreover, the production-based availability

is calculated as follows:

$$A_{\text{prod}} = 1 - \frac{\text{Lost production}}{\text{Actual energyproduction} + \text{Lost production}}. \tag{17}$$

Furthermore, the reliability of a generation system, here a WF, can be measured by the expected energy not produced (EENP) due to the unavailability of WF components [60] as follows:

$$\text{EENP} = \sum_{i=1}^{n} \Psi_i \cdot \left(P_i^A - P_i^u\right) \cdot 8760 \tag{18}$$

where Ψ_i is the WF capacity in state i, P_i^A is the probability of state i considering the WF components are fully available and P_i^u is the probability of state i considering the unavailability of the WF components.

F. Reliability of Power System

Power system reliability is measured by probabilistic indices such as LOLE and EENS [30], [45]. These two indices are the most popular measures of power system adequacy, where the LOLE is the number of days or hours within a specific period of time in which the load cannot be supplied due to the generation shortage, and it is calculated as follows:

$$\text{LOLE} = \sum_{i=1}^{n} P_i \cdot (C_i - L_i) \tag{19}$$

where C_i is the available capacity in interval i, L_i is the forecast peak load, P_i is the portability of loss of load [30]. EENS is also defined as the curtailed energy due to the generation shortage and it is estimated by using the following equation [61]:

$$\text{EENS} = \sum_{i=1}^{n} P_i \cdot E_i \tag{20}$$

where E_i is the curtailed energy.

The flow of the reliability prediction in the power system is shown in Fig. 9. First, the wear-out failure rate of power converters of WT is predicted accordingly on SSA under a given mission profile for each WT. Afterward, the WTC availability is estimated based on wear-out and random chance failure rates. Then, the availability of WT is estimated according to the availability of the WT components and wind power availability. The WF HVDC transmission line availability can also be predicted based on converters wear-out failure and historical data of random chance failures. Combining the availability of the WTs and the WF transmission line will result in the WF reliability model and its availability. Furthermore, the HVDC transmission system availability can also be predicted based on the availability of transmission line reliability which is obtained by converters wear-out random chance failures. The availability of conventional generators can also be modeled based on the availability of individual units according to [30]. The overall generation system reliability model can be obtained by combining the reliability models of WFs, HVDC systems and conventional generators. Finally,

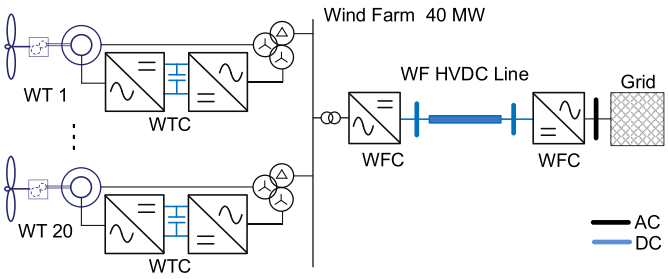

Fig. 8. 40-MW DFIG-based WF structure with 20 × 2 MW WTs.

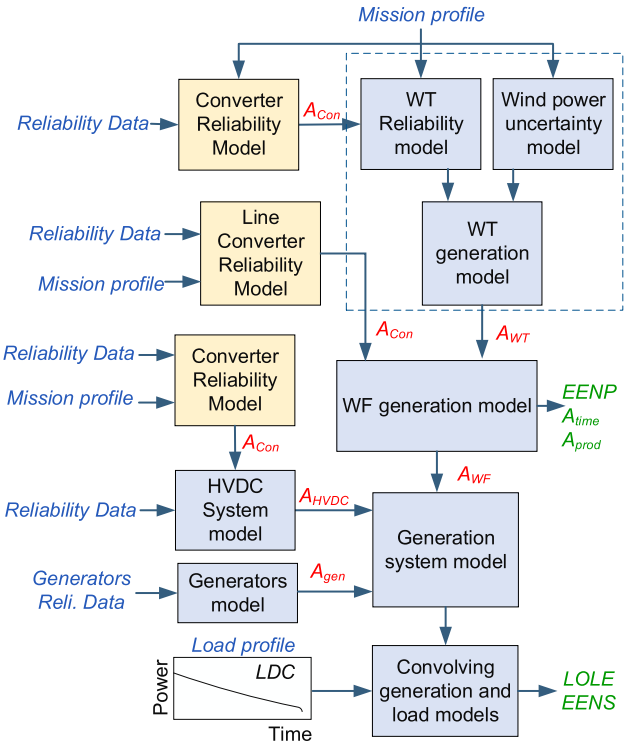

Fig. 9. Reliability evaluation in modern power systems.

the system reliability indices including LOLE and EENS are predicted by convolving the generation system reliability and the system load model.

V. Numerical Analysis

In modern power systems, the energy sources can be conventional generators, WTs, solar photovoltaic arrays, energy storage systems, and neighboring grids. In this article, the reliability of two power system structures is evaluated. The first system is the modified Roy Billinton Test System (RBTS) with additional 40 MW and 4 × 40 MW WFs with 20% and 64% wind penetration, respectively. The structure of the modified RBTS is shown in Fig. 10. The RBTS information including reliability data and load model are provided in [62]. The structure of the 40-MW WF is shown in Fig. 8 including 20 2-MW V80-2.0 WTs manufactured by Vestas wind turbine system with cut-in, rated, and cut-out speeds of 4, 15, and 25 m/s, respectively. The WF is connected to the grid through a dc transmission line. Wind speed data of two different

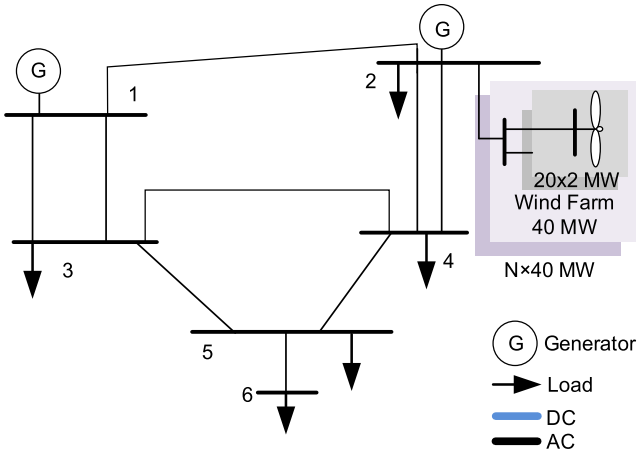

Fig. 10. Modified RBTS (the main version is provided in [62]), WFC.

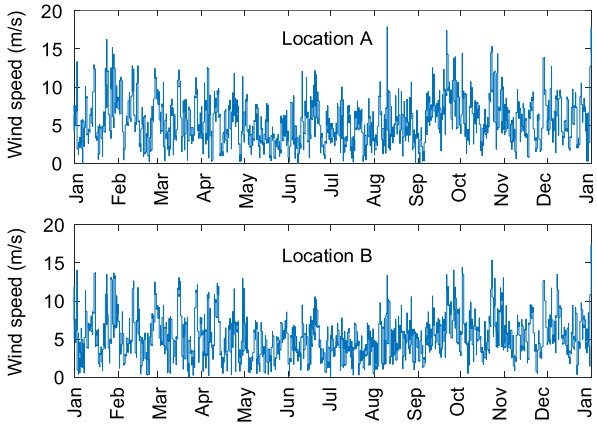

Fig. 11. Wind speed profile of two locations with one-minute resolution.

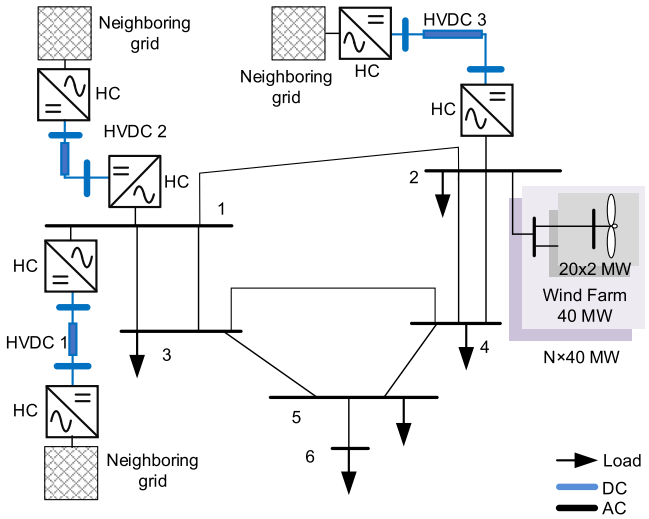

Fig. 12. Full PE-RBTS. HC: HVDC converter.

locations with resolution of one minute is utilized as shown in Fig. 11.

Moving toward 100% renewable energies necessitates the power systems to interconnect into the neighboring grids.

TABLE I

WF RELIABILITY INDICES FOR THE BASE CASE GIVEN IN THE APPENDIX

WF	U_{time} [h/y]	A_{prod} [%]	EENP [MWh/y]
160 MW	168	97	18,550

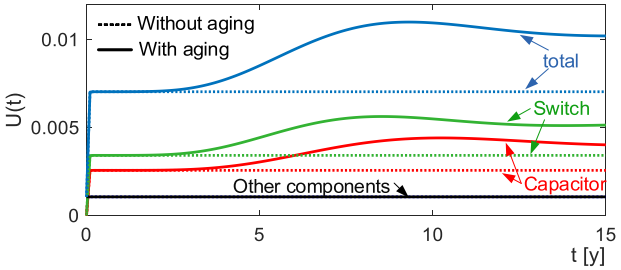

Fig. 13. Impact of component aging on the converter unavailability, U(t). $(\alpha, \beta)_{switch} = (12, 3)$ and $(\alpha, \beta)_{cap} = (10, 3)$.

Therefore, the RBTS is further modified by interconnecting to the neighboring grids through three 100-MW HVDC lines as shown in Fig. 12. The modified RBTS is fully equipped with PE, and it would be called modified PE-RBTS. In this case, it is assumed that the neighboring grids are always available, and the local grid does not support the neighboring grids. In the following, the reliability of the two power systems is analyzed.

A. Converter Availability

The converter availability (or unavailability) depends on the random chance and wear-out failure rates. The random chance failure rate of converters is provided in Appendix. Moreover, the wear-out failure rate is predicted based on SSA for the WTC shown in Fig. 8 under the given mission profiles in Fig. 11. The converter structure and characteristics for a 2-MW doubly-fed induction generator (DFIG)-based WT is provided in [63] which includes a 0.4-MW partial-scale two-level converter. Since the thermal modeling and SSA of converters have been widely addressed in [18], [22], [47], [63], and [64], the detailed modeling process is not represented here. Hence, the reliability prediction is carried out following the procedure described in Fig. 3, and the results are employed for system-level analysis. The wear-out failure rates are represented by a Weibull distribution as given in (6). Following the SSA-based reliability prediction approach, the wear-out failure rate characteristics of the converter switches and capacitors are obtained as $(\alpha, \beta)_{switch} = (12, 3)$, $(\alpha, \beta)_{cap} = (10, 3)$ for the mission profile of location A and $(\alpha, \beta)_{switch} = (8, 3)$, $(\alpha, \beta)_{cap} = (7, 2.6)$ for location B.

The converter components unavailability is predicted for both constant and time-varying failure rates using (9). Their unavailability due to the random chance failures and the total unavailability are shown in Fig. 13. The total converter unavailability due to the random chance failures is almost 0.007. It can be seen from Fig. 13 that the wear-out of converter components will increase its unavailability from 0.007 to 0.011 shape factors (α, β). As a result, employing the random

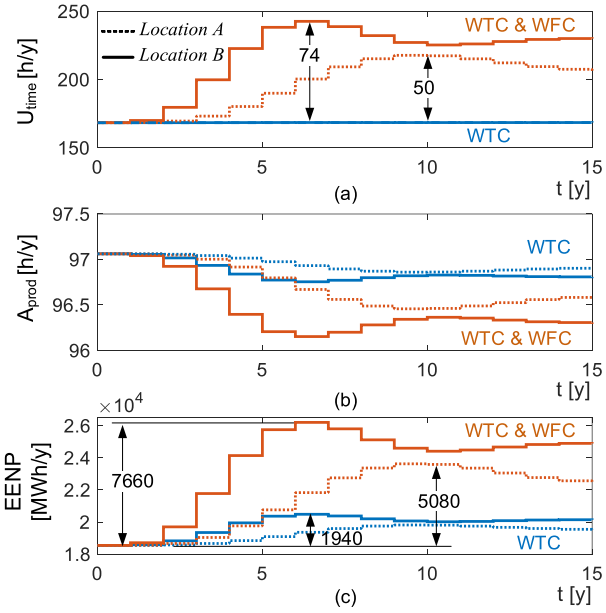

Fig. 14. Impact of WTC and WFC wear out on the reliability of 160-MW WF. (a) Time-based unavailability. (b) Production-based availability. (c) EENP due to the wear out of WFC or WTC.

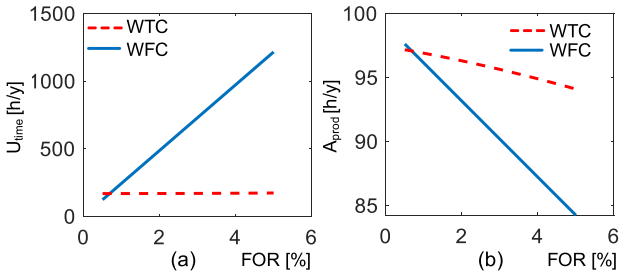

Fig. 15. Impact of WTC and WFC unavailability (FOR) on the (a) time-based unavailability and (b) production-based availability of the WF.

chance failure rate and neglecting the impact of components aging will introduce error on the converter reliability. The unavailability of the HCs of WF and transmission systems in the modified RBTS can be predicted similar to this case, and the total unavailability can be used for system-level analysis.

B. WF Reliability

The WF reliability is evaluated employing the historical reliability data summarized in Appendix as a base case. These data are associated with random chance failures. For the base case, the reliability indices are summarized in Table I, where the time-based unavailability is 168 h/year, the production-based availability is 97.0% and the EENP is equal to 18 550 MWh/year.

The impact of converter components wear-out on the performance of the 4 × 40 MW WF is illustrated in Fig. 14. The wear-out characteristics of WTC under two mission profiles is $(\alpha,\ \beta)_{\text{switch}} = (12, 3)$, $(\alpha,\ \beta)_{\text{cap}} = (10, 3)$ for location A and $(\alpha,\ \beta)_{\text{switch}} = (8,\ 3)$, $(\alpha,\ \beta)_{\text{cap}} = (7,\ 2.6)$ for location B. Moreover, for the WFC, the components wear-out characteristics is assumed to be $(\alpha,\ \beta)_{\text{switch}} = (\alpha,\ \beta)_{\text{cap}} = (12,\ 3)$, and $(\alpha,\ \beta)_{\text{switch}} = (\alpha,\ \beta)_{\text{cap}} = (8,\ 3)$, respectively, for locations A and B. According to Fig. 14(a) and (b), the impact of WTC on the time-based unavailability and production-based availability is negligible. Also, the impact of WFC on the time-based unavailability is 74 h/year higher than the base case (168 h/year) in Location B as shown in Fig. 14(a). Therefore, ignoring the impact of WFC and using the historical reliability data will introduce almost 44% error in time-based unavailability prediction following Fig. 14(a).

Furthermore, as is shown in Fig. 14(a), the aging parameters of the WFC can affect the unavailability of the WF, whereby decreasing α from 12 in location A to 8 in location B, the maximum time-based unavailability is increased from 218 to 242 h/year. The EENP of the WF is illustrated in Fig. 14(c) highlighting the impact of converters wear-out. The aging of WTC will introduce 1940 MWh/year EENP over the base case which is almost 10%. Furthermore, wear-out of WTCs and WFCs causes 5080 MWh/year in location A and 7660 MWh/year in location B more EENP compared to the base case, which are equal to 27% and 41% of the base case, respectively.

The results in Fig. 14 show that the different WF availability measures are not identical, and may not appropriately show the WF performance. For instance, the impact of WTC wear-out on the time-based unavailability is almost negligible while it can introduce 10% more EENP over the base case. Furthermore, the aging parameters of WTCs and WFCs can affect the reliability of the WF, and thus, need to be modeled in the system-level analysis. However, the impact of WFC wear-out is much higher than the impact of WTC. This case study shows that the wind speed profile can affect the converters reliability, and hence, the WF availability. Thus, modeling the converters aging in the system-level analysis is of high importance.

Since the converter failure rate is dependent on the operational and environmental conditions, a senility analysis is performed to show the impact of random chance failure rates on the overall performance of WF. Notably, during the sensitivity analysis on the FOR of one of the WTC or WFC, the FOR of the other one is kept constant at the base case as given in Appendix. Following Fig. 15(a), the FOR of WTC does not affect the time-based unavailability and its impact on the production-based availability is almost negligible as shown in Fig. 15(b). Meanwhile, the WFC considerably affects the time-based unavailability and production-based unavailability of the WF reliability as shown in Fig. 15.

Furthermore, the EENP of a 40 MW and 4 × 40 MW WFs are calculated for the base case which is equal to 4.64 and 18.55 GWh/year, respectively. The impact of converters FOR is reported in Fig. 16(a) and (b), respectively. The results show that increasing the WFC FOR remarkably increases the WF EENP, while the impact of WTC on the EENP is not considerable.

C. Power System Reliability

The reliability of modified RBTS and PE-RBTS is evaluated by LOLE and EENS indices. The base case reliability indices

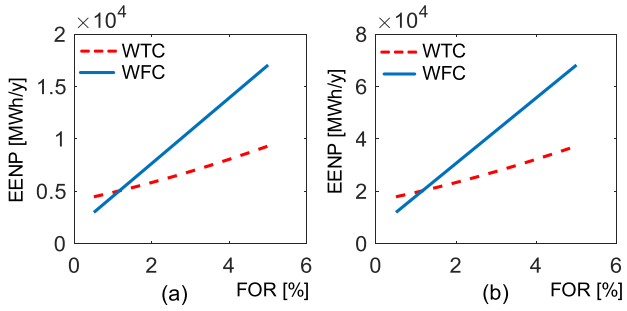

Fig. 16. Impact of WTC and WFC unavailability (FOR) on the EENP by the (a) 40-and (b) 160-MW WF.

TABLE II
RELIABILITY INDICES OF POWER SYSTEM FOR THE BASE CASE GIVEN IN THE APPENDIX

SYSTEM	RBTS			PE-RBTS
WF Capacity [MW]	0	40	160	160
PLCC [MW]	0	16	65	65
Peak load [MW]	185	201	250	250
Wind penetration [%]	0	20	64	64
LOLE [h/y]	1.14	1.24	1.31	4.10
EENS [MWh/y]	10.00	9.57	12.48	165.00

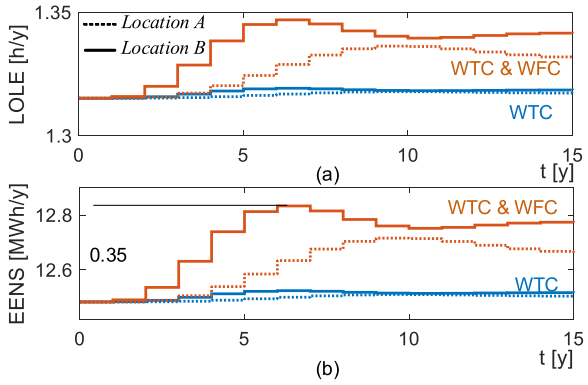

Fig. 17. Impact of WTC and WFC wear out on the reliability of RBTS with 160-MW WF. (a) LOLE. (b) EENS.

are summarized in Table II. The LOLE of the RBTS is 1.14 h/year. In order to approximately keep the LOLE to be identical to the base case, the peak load of the system is increased accordingly. This incremental peak load, which is called peak load carrying capability (PLCC), for modified RBTS is reported in Table II. Furthermore, the PLCC for the EP-RBTS is considered as the case of RBTS with 160-MW WF, since the wind capacity penetration in both cases is identical.

1) Modified RBTS Reliability: The impact of WTC and WFC wear-out failure on the system reliability is illustrated in Fig. 17 with the 160-MW WF. First, the aging of WTCs is considered. Following Fig. 17, the WTCs wear-out has negligible impact on the system LOLE and EENS. Next, the aging of both WTCs and WFC is modeled. The obtained results in Fig. 17 show that the converters aging impact on the LOLE is 2% and EENS is 3%. As a result, for power

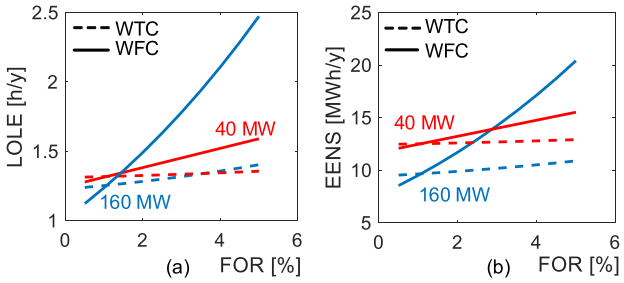

Fig. 18. Impact of WTC and line converter unavailability (FOR) on the (a) LOLE and (b) EENS in RBTS with 40- and 160-MW WF.

system-level analysis, the WTCs and WFCs wear-out failure impacts can be neglected.

Moreover, the impact of WTCs and WFCs FOR on the RBTS reliability is shown in Fig. 18(a) and (b) with the 40- and 160-MW WFs. The sensitivity analysis is performed on the FOR of one of the WTC or WFC, while the FOR of the other one is assumed to be constant as given in Appendix. As can be seen in Fig. 18, increasing the WTC FOR cannot affect the LOLE and EENS with low and high penetration of wind power. However, the system reliability is dependent on the WFC FOR and wind power penetration. As can be seen in Fig. 18(a), by increasing the WFC FOR with 40-MW WF, the change of LOLE is almost negligible. However, with the 160-MW WF, the impact of WFC FOR on the LOLE is significant as shown in Fig. 18(a). The impact of FOR of converters on the EENS is also similar to the LOLE as shown in Fig. 18(b). Therefore, the WTCs impact on the system reliability is almost negligible, while the WFCs can affect the system reliability especially with high wind power penetration. Thus, the appropriate reliability data of WFCs should be employed in the system-level reliability assessment.

2) Modified PE-RBTS Reliability: The reliability of the full power electronic-based system, PE-RBTS shown in Fig. 12 is evaluated in this section. The base case reliability indices have been summarized in Table II. Following these results, replacing the conventional generators with HVDC systems connected to the neighboring grids, the base LOLE is increased from 1.31 to 4.10 h/year. Moreover, the system EENS is increased from 12.38 to 165.00 MWh/year. Therefore, moving to full power electronic systems requires HVDC systems with high availability in order to obtain the same performance as the conventional systems.

In order to illustrate the impact of HC aging on the system reliability, the wear-out characteristics of HC converter components are assumed to be $(\alpha,\ \beta)_{\text{switch}} = (\alpha,\ \beta)_{\text{cap}} = (8,\ 3)$. The PE-RBTS LOLE and EENS due to the wear-out failure of WFCs and HCs are shown in Fig. 19. The HCs aging increases the LOLE by 4.5 h/year (109%) and EENS by 190 MWh/year (115%) as shown in Fig. 19(a) and (b). However, the WFCs wear-out impact on LOLE and EENS is negligible.

Moreover, the impact of FOR of HCs and WFCs with 160-MW WF with wind capacity penetration of 65% is shown in Fig. 20. As can be seen from Fig. 20, the LOLE and EENS

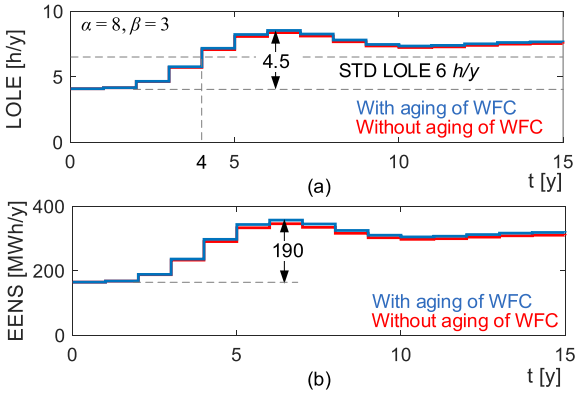

Fig. 19. Impact of WFC and HC wear out on the reliability of PE-RBTS with 160-MW WF. (a) LOLE. (b) EENS.

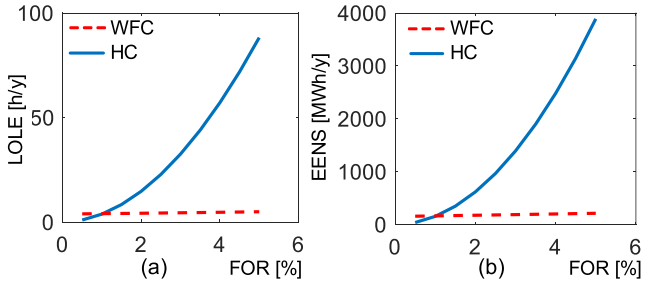

Fig. 20. Impact of WTC and WFC unavailability (FOR) on the (a) LOLE and (b) EENS in PE-RBTS with 40- and 160-MW WF.

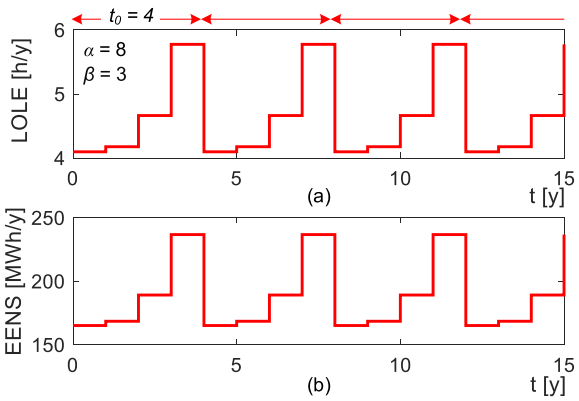

Fig. 21. Impact of the age replacement policy of HC on the reliability of PE-RBTS with 160-MW WF. (a) LOLE. (b) EENS.

are significantly affected by the HC FOR, while the impact of WFCs is negligible. Notably, the WFC FOR is kept constant as given in Appendix within analyzing the impact of HC FOR and vice versa. The obtained results show that the random-chance and wear-out failure rate of HC components have a significant impact on the overall system reliability.

Therefore, in a full power electronic-based power system, accurate reliability analysis requires utilizing appropriate reliability data for random chance failures that must be utilized. Moreover, the detailed wear-out failure rate of HC components must be predicted in order to accurately analyze the system reliability. Ignoring the aging of components may introduce erroneous results, consequently nonoptimal decision-making within planning and operation of such systems.

3) Impact of Replacement Policy: The LOLE index in a reliable power system must be limited to a standard value, which depends on every country's regulations. For instance, its standard value for European countries is between 4 and 8 h/year [46]. Considering the standard level of 6 h/year, the system performance with the run-to-fail maintenance strategy is not acceptable as shown in Fig. 19(a). Therefore, a proper maintenance strategy such as an age replacement policy must be adopted in order to maintain the system reliability. According to the age replacement policy, the components will be replaced upon failure or specific time t_o, whichever comes first. Following the system performance shown in Fig. 19(a), the appropriate time of replacement based on the age replacement policy would be the cross points of LOLE cures with the standard level of 6 h/year. As can be seen from Fig. 19(a), the appropriate planned replacement time t_o, would be four years. As a result, applying the age replacement policy at the planned times, the overall system reliability can be obtained as shown in Fig. 21. It is clear that the time of planned replacement scheduling depends on the wear-out failure characteristics of the HC converters. Therefore, accurate wear-out failure prediction of converters is necessary for appropriate maintenance scheduling in modern power systems.

VI. Discussion

The converters are utilized in generation systems such as for wind and solar energy resources, and electronic transmission systems such as HVDC lines. Hence, the converter reliability may affect the overall system reliability according to its applications. Meanwhile, the converters are fragile components and particularly they are prone to aging failures. Thereby, this article has explored the impact of converter failures on the modern power electronic-based power systems performance. First, the wear-out failure prediction based on SSA in power converters has been presented. Next, the converter reliability model has been incorporated into the power system analysis. Finally, the reliability evaluation in modern power systems has been presented. The impact of converters reliability on the modified RBTS with different proliferation of power converters has been illustrated.

It has been shown that the wear-out failures can affect the converter availability according to the aging parameters. The impact of converter availability on the WF reliability has been illustrated with 20% and 64% wind power penetration. The obtained results have shown that the WTC has a negligible impact on the time-based unavailability and production-based availability of WFs. However, its wear-out failure may increase the EENP by 10% compared to the case of neglecting the wear-out failures. Furthermore, the WFC can highly affect the WF reliability indices. The analysis has shown that the wear-out failure of WFC may introduce almost 45% unavailability over the base case. As a result, the WFC reliability considering the random chance and wear-out failures must accurately be modeled for reliability prediction of WFs. Since, the number of these converters is not too much, e.g., two converters

per 40-MW WF, hence, its reliability modeling based on SSA might not be time-consuming. However, the number of WTCs is quite high, e.g., 2 × 40 converters in a 40-MW WF. Thereby, its reliability modeling, especially considering different mission profiles for each WT in practice, is almost impossible. As a result, considering the time of analysis with high penetration of WFs, the wear-out reliability of WTCs can be neglected, while it can induce 10% error in the results.

The impact of WTCs and WFCs on the reliability of RBTS with 20% and 64% of wind power penetration has been evaluated. It has been shown that the impact of WTCs and WFCs failures including random chance and wear-out failures on the LOLE and EENS in low and high wind power penetration is almost negligible. Thus, the SSA-based wear-out analysis for the system-level studies for both WTCs and WFCs may not be necessary. However, the WFC FOR can affect the system reliability in high wind power penetration. Therefore, for system reliability analysis, the WFC FOR due to the random chance failures must be appropriately adopted from operation experiences and historical data.

Finally, a modified version of RBTS as a full power electronic system, PE-RBTS is considered with three HVDC links connected to the neighboring countries. The obtained results have shown that the reliability of the system significantly depends on the HVDC system availability. Furthermore, the wear-out failure of HCs has a remarkable impact on the overall system reliability. Therefore, the HC reliability, especially the wear-out failures, must be accurately modeled for the system-level analysis. Furthermore, the impact of run-to-fail and age replacement polices for HCs has been shown in this article, where the age replacement policy at a proper time is required to maintain the system reliability under a standard limit.

This article bridged the reliability concept of power electronic converters and power systems. It presented a method to model the reliability of electronic-based power systems from device-level up to power system-level. Moreover, the impact of power converters on the system reliability at different applications with different penetration level of renewable (wind) energies was illustrated. In the analysis, the wind profile for all WTs are considered to be identical. The impact of wind regime with different wind profile of WTs on the converter and WF and power system reliability will be analyzed in the future. Furthermore, the neighboring networks are assumed to be a back-up to support the grid security. The future work will be focused on the full renewable energy grids with energy storage systems, where all the energy sources are equipped with power electronic converters. Hence, the impact of long-term energy management system and storage system converter on overall system reliability should be explored.

VII. Conclusion

This article has proposed a procedure to bridge the power electronic and power system reliability concepts. The reliability of power electronic converters is incorporated in power system reliability analysis, which can be beneficial for optimal decision-making within planning, operation, and maintenance of modern power systems. The detailed reliability modeling of power electronic-based power systems has been presented from the device-level up to the power system-level. The impact of converter failure rates on power system performance has been illustrated for different applications. For instance, it has been shown that the wear-out failure of WTC cannot affect the WF and power system performance even under run-to-fail replacement strategy. Moreover, since the converter reliability modeling in electrothermal domains is a time-consuming process, the required accuracy in reliability modeling of power converters for different applications has been addressed. This can facilitate the system-level reliability evolution on modern power systems with the high proliferation of power converters. Furthermore, the impact of run-to-fail and age replacement polices for power converters on the overall system reliability has been illustrated.

The reliability assessment approach can be easily performed for photovoltaic systems by appropriately modeling the availability of solar energy. The remaining analysis will be similar to wind power plants. Future research will focus on the impact of power management strategies on the system-level reliability of converters. Moreover, appropriate maintenance strategies could be introduced for different applications of converters in power systems.

TABLE III
Exponential Failure and Repair Rates of WT and HVDC System [3], [36], [37], [65], and [66]

Unit	Sub-system	Component	Failure rate [occ/y]	Repair rate [r/y]
WT	Converter (con.)	Switch	0.15	150
		Capacitor	0.2	150
		Other con. comp.	0.15	185
	Other	Other WT comp.	0.53	200
HVDC	Converter (con.)	Switch	0.3	200
		Capacitor	0.43	50
		Other con. comp.	0.35	10
	Other Comp.	DC Line	0.003	17

Appendix

The reliability data for base case used in this article are summarized in Table III which are based on the data provided in [3], [36], [37], [65], and [66].

References

[1] J. H. Enslin, S. G. Whisenant, and R. Hadidi, "Third egrid workshop maps the grid of the future: Attendees engage to examine the role of power electronic applications in modern electric power systems," *IEEE Power Electron. Mag.*, vol. 6, no. 1, pp. 48–55, Mar. 2019.

[2] S. Yang, A. Bryant, P. Mawby, D. Xiang, L. Ran, and P. Tavner, "An industry-based survey of reliability in power electronic converters," *IEEE Trans. Ind. Appl.*, vol. 47, no. 3, pp. 1441–1451, May 2011.

[3] J. Ribrant and L. M. Bertling, "Survey of failures in wind power systems with focus on Swedish wind power plants during 1997–2005," *IEEE Trans. Energy Convers.*, vol. 22, no. 1, pp. 167–173, Mar. 2007.

[4] K. Fischer *et al.*, "Reliability of power converters in wind turbines: Exploratory analysis of failure and operating data from a worldwide turbine fleet," *IEEE Trans. Power Electron.*, vol. 34, no. 7, pp. 6332–6344, Jul. 2019.

[5] J. Carroll, A. Mcdonald, and D. Mcmillan, "Reliability comparison of wind turbines with DFIG and PMG drive trains," *IEEE Trans. Energy Convers.*, vol. 30, no. 2, pp. 663–670, Jun. 2015.

[6] X. Liu and S. Islam, "Reliability issues of offshore wind farm topology," in *Proc. 10Th Int. Conf. Probabilistic Methods Appl. To Power Syst.*, 2008, pp. 523–527.

[7] G. J. W. Van Bussel and M. B. Zaaijer, "DOWEC concepts study, reliability, availability and maintenance aspects," in *Proc. Eur. Wind Energy Conf.*, Jul. 2001, pp. 557–560.

[8] L. M. Moore and H. N. Post, "Five years of operating experience at a large, utility-scale photovoltaic generating plant," *Prog. Photovolt., Res. Appl.*, vol. 16, no. 3, pp. 249–259, May 2008.

[9] G. Zini, C. Mangeant, and J. Merten, "Reliability of large-scale grid-connected photovoltaic systems," *Renew. Energy*, vol. 36, no. 9, pp. 2334–2340, Sep. 2011.

[10] A. Golnas, "PV system reliability: An operator's perspective," *IEEE J. Photovolt.*, vol. 3, no. 1, pp. 416–421, Jan. 2013.

[11] L. Alhmoud, "Reliability improvement for a high-power IGBT in wind energy applications," *IEEE Trans. Ind. Electron.*, vol. 65, no. 9, pp. 7129–7137, Sep. 2018.

[12] H. S. Chung, H. Wang, F. Blaabjerg, and M. Pecht, *Reliability of Power Electronic Converter Systems*, 1st ed. London, U.K.: IET, 2016.

[13] F. Spinato, P. Tavner, G. Van Bussel, and E. Koutoulakos, "Reliability of wind turbine subassemblies," *IET Renew. Power Gener.*, vol. 3, no. 4, p. 387, 2009.

[14] S. Peyghami, P. Davari, and F. Blaabjerg, "System-level reliability-oriented power sharing strategy for DC power systems," *IEEE Trans. Ind. Appl.*, vol. 55, no. 5, pp. 4865–4875, Sep. 2019.

[15] Y. Song and B. Wang, "Survey on reliability of power electronic systems," *IEEE Trans. Power Electron.*, vol. 28, no. 1, pp. 591–604, Jan. 2013.

[16] F. Blaabjerg, K. Ma, and D. Zhou, "Power electronics and reliability in renewable energy systems," in *Proc. IEEE Int. Symp. Ind. Electron.*, May 2012, pp. 19–30.

[17] H. Wang, K. Ma, and F. Blaabjerg, "Design for reliability of power electronic systems," in *Proc. IEEE IECON*, Jan. 2012, pp. 33–44.

[18] P. D. Reigosa *et al.*, "Prediction of bond wire fatigue of IGBTs in a PV inverter under a long-term operation," *IEEE Trans. Power Electron.*, vol. 31, no. 10, pp. 3052–3059, Mar. 2016.

[19] J. Falck, C. Felgemacher, A. Rojko, M. Liserre, and P. Zacharias, "Reliability of power electronic systems: An industry perspective," *EEE Ind. Electron. Mag.*, vol. 12, no. 2, pp. 24–35, Jun. 2018.

[20] K. Ma and F. Blaabjerg, "Modulation methods for neutral-point-clamped wind power converter achieving loss and thermal redistribution under low-voltage ride-through," *IEEE Trans. Ind. Electron.*, vol. 61, no. 2, pp. 835–845, Feb. 2014.

[21] Y. Wu, M. A. Shafi, A. M. Knight, and R. A. Mcmahon, "Comparison of the effects of continuous and discontinuous PWM schemes on power losses of voltage-sourced inverters for induction motor drives," *IEEE Trans. Power Electron.*, vol. 26, no. 1, pp. 182–191, Jan. 2011.

[22] S. Peyghami, H. Wang, P. Davari, and F. Blaabjerg, "Mission-profile-based system-level reliability analysis in DC microgrids," *IEEE Trans. Ind. Appl.*, vol. 55, no. 5, pp. 5055–5067, Sep. 2019.

[23] M. Andresen, G. Buticchi, and M. Liserre, "Study of reliability-efficiency tradeoff of active thermal control for power electronic systems," *Microelectron. Rel.*, vol. 58, pp. 119–125, Mar. 2016.

[24] K. Ma, "Reactive power influence on the thermal cycling of multi-MW wind power inverter," *IEEE Trans. Ind. Appl.*, vol. 49, no. 2, pp. 922–930, Mar./Apr. 2013.

[25] Z. Qin, M. Liserre, F. Blaabjerg, and H. Wang, "Energy storage system by means of improved thermal performance of a 3 MW grid side wind power converter," in*Proc. IEEE IECON*, Nov. 2013, pp. 736–742.

[26] Z. Qin, M. Liserre, F. Blaabjerg, and P. Chiang Loh, "Reliability-oriented energy storage sizing in wind power systems," in *Proc. Int. Power Electron. Conf. (IPEC-ECCE ASIA)*, May 2014, pp. 857–862.

[27] S. Peyghami, P. Davari, H. Wang, and F. Blaabjerg, "System-level reliability enhancement of DC/DC stage in a single-phase PV inverter," *Microelectron. Rel.*, vols. 88–90, pp. 1030–1035, Sep. 2018.

[28] S. Peyghami, P. Davari, H. Wang, and F. Blaabjerg, "The impact of topology and mission profile on the reliability of boost-type converters in PV applications," in *Proc. IEEE 19th Workshop Control Model. for Power Electron. (COMPEL)*, Jun. 2018., pp. 1–8.

[29] V. Raveendran, M. Andresen, and M. Liserre, "Improving onboard converter reliability for more electric aircraft with lifetime-based control," *IEEE Trans. Ind. Electron.*, vol. 66, no. 7, pp. 5787–5796, Jul. 2019.

[30] L. Lightfoot, "Reliability evaluation of power systems," *Electron. Power UK*, vol. 30, no. 6, p. 483, 1984.

[31] A. Kwasinski, "Quantitative evaluation of DC microgrids availability: Effects of system architecture and converter topology design choices," *IEEE Trans. Power Electron.*, vol. 26, no. 3, pp. 835–851, Mar. 2011.

[32] S. Sulaeman, M. Benidris, J. Mitra, and C. Singh, "A wind farm reliability model considering both wind variability and turbine forced outages," *IEEE Trans. Sustain. Energy*, vol. 8, no. 2, pp. 629–637, Apr. 2017.

[33] H. J. Bahirat, G. H. Kjolle, B. A. Mork, and H. K. Hoidalen, "Reliability assessment of DC wind farms," in *Proc. IEEE Power Energy Soc. General Meeting*, Jul. 2012, pp. 1–7.

[34] P. Wang, Z. Gao, and L. Bertling, "Operational adequacy studies of power systems with wind farms and energy storages," *IEEE Trans. Power Syst.*, vol. 27, no. 4, pp. 2377–2384, Nov. 2012.

[35] A. S. Dobakhshari and M. Fotuhi-Firuzabad, "A reliability model of large wind farms for power system adequacy studies," *IEEE Trans. Energy Convers.*, vol. 24, no. 3, pp. 792–801, Sep. 2009.

[36] Y. Guo, H. Gao, and Q. Wu, "A combined reliability model of VSC-HVDC connected offshore wind farms considering wind speed correlation," *IEEE Trans. Sustain. Energy*, vol. 8, no. 4, pp. 1637–1646, Oct. 2017.

[37] S. Zadkhast, M. Fotuhi-Firuzabad, F. Aminifar, R. Billinton, S. O. Faried, and A.-A. Edris, "Reliability evaluation of an HVDC transmission system tapped by a VSC station," *IEEE Trans. Power Del.*, vol. 25, no. 3, pp. 1962–1970, Jul. 2010.

[38] B. Jacobson, K. Linden, J. Lundquist, and M. H. J. Bollen, "Reliability study methodology for HVDC grids," Working Group CIGRE B4-108_2010, Aug. 2010, pp. 1–10.

[39] H. Yang, Z. Cai, X. Li, and C. Yu, "Assessment of commutation failure in HVDC systems considering spatial-temporal discreteness of AC system faults," *J. Mod. Power Syst. Clean Energy*, vol. 6, no. 5, pp. 1055–1065, Sep. 2018.

[40] L. Shen, Q. Tang, T. Li, Y. Wang, and F. Song, "A review on VSC-HVDC reliability modeling and evaluation techniques," *IOP Conf. Ser., Mater. Sci. Eng.*, vol. 199, May 2017, Art. no. 012133.

[41] C. Maciver, K. R. W. Bell, and D. P. Nedic, "A reliability evaluation of offshore HVDC grid configuration options," *IEEE Trans. Power Del.*, vol. 31, no. 2, pp. 810–819, Apr. 2016.

[42] C. K. Kapur and M. Pecht, *Reliability Engineering*, 1st ed. Hoboken, NJ, USA: Wiley, 2014.

[43] R. Billinton and R. Allan, *Reliability Evaluation of Engineering Systems*. New York, NY, USA: Plenum Press, 1992.

[44] S. Peyghami, P. Davari, M. Fotuhi-Firuzabad, and F. Blaabjerg, "Standard test systems for modern power system analysis: An overview," *IEEE Ind. Electron. Mag.*, vol. 13, no. 4, pp. 86–105, Dec. 2019.

[45] R. Billinton and K. Chu, "Early evolution of LOLP: Evaluating generating capacity requirements [history]," *IEEE Power Energy Mag.*, vol. 13, no. 4, pp. 88–98, Jul. 2015.

[46] M. Ćepin and M. Cepin, *Assessment of Power System Reliability Methods and Applications*. New York, NY, USA: Springer, 2011.

[47] S. Peyghami, Z. Wang, and F. Blaabjerg, "Reliability modeling of power electronic converters: A general approach," in *Proc. 20th Workshop Control Model. Power Electron. (COMPEL)*, Jun. 2019, pp. 1–7.

[48] *Reliability Data Handbook-Universal Model for Reliability Prediction of Electronics Components*, document IEC TR 62380, PCBs and Equipment, 2006.

[49] (2010). *FIDES Guide 2009 Edition: A Reliability Methodology for Electronic Systems*. Accessed: Feb. 2, 2019. [Online]. Available: https://www.fides-reliability.org/

[50] A. Albertsen, "Electrolytic capacitor lifetime estimation," in *Proc. JIANGHAI Eur. GmbH*, 2010, pp. 1–13.

[51] R. Bayerer, T. Herrmann, T. Licht, J. Lutz, and M. Feller, "Model for power cycling lifetime of IGBT modules—Various factors influencing lifetime," in *Proc. IEEE CIPS*, Mar. 2008, pp. 1–6.

[52] A. Wintrich *et al.*, *Application Manual Power Semiconductors*, 2nd ed. Berlin, Germany: ISLE Verlag, 2015.

[53] *The Future Of Reliability—Definition Of Reliability In Light Of New Developments in Various Devices And Services Which Offer Customers And System Operators New Levels Of Flexibility*, Cigre Working Group (WG C1.27), CIGRE, 2018.

[54] W. R. Nunn and A. M. Desiderio, "Semi-Markov processes: An introduction," in *Proc. Cent. Nav. Anal.*, Jul. 1977, pp. 1–30.

[55] A. Lisnianski, I. Frenkel, Y. Ding, A. Lisnianski, I. Frenkel, and Y. Ding, *Multi-State System Reliability Analysis and Optimization for Engineers and Industrial Managers*. London, U.K.: Springer, 2010.
[56] F. Bhuiyan and A. Yazdani, "Reliability assessment of a wind-power system with integrated energy storage," *IET Renew. Power Gener.*, vol. 4, no. 3, p. 211, 2010.
[57] *Part 26-1: Time-Based Availability for Wind Turbine Generating Systems*, document IEC61400-26-1, 2011.
[58] *Part 26-2: Production-Based Availability for Wind Turbines*, document IEC61400-26-2, 2014.
[59] *Part 26-3: Availability for Wind Power Stations*, document IEC61400-26-3, 2016.
[60] Y. Makarov, "Probabilistic assessment of the energy not produced due to transmission constraints," in *Proc. IEEE Bologna Power Tech. Conf.*, Jul. 2004, pp. 435–437.
[61] R. Billinton and P. G. Harrington, "Reliability evaluation in energy limited generating capacity studies," *IEEE Trans. Power App. Syst.*, vols. PAS–97, no. 6, pp. 2076–2085, Nov. 1978.
[62] R. Billinton *et al.*, "A reliability test system for educational purposes-basic data," *IEEE Power Eng. Rev.*, vol. 9, no. 8, pp. 67–68, Aug. 1989.
[63] D. Zhou, F. Blaabjerg, M. Lau, and M. Tonnes, "Thermal cycling overview of multi-megawatt two-level wind power converter at full grid code operation," *IEE J. Int. Appl.*, vol. 2, no. 4, pp. 173–182, 2013.
[64] K. Ma, M. Liserre, F. Blaabjerg, and T. Kerekes, "Thermal loading and lifetime estimation for power device considering mission profiles in wind power converter," *IEEE Trans. Power Electron.*, vol. 30, no. 2, pp. 590–602, Feb. 2015.
[65] B. Hahn, M. Durstewitz, and K. Rohrig, "Reliability of wind turbines—Experience of 15 years with 1500WTs," in *Euromech Colloquium*. Berlin, Germany: Springer-Verlag, 2005, pp. 329–332.
[66] C. J. Crabtree, D. Zappalá, and S. I. Hogg, "Wind energy: UK experiences and offshore operational challenges," *Proc. Inst. Mech. Eng., A, J. Power Energy*, vol. 229, no. 7, pp. 727–746, Nov. 2015.

Saeed Peyghami (Member, IEEE) received the B.Sc., M.Sc., and Ph.D. degrees in electrical engineering from the Department of Electrical Engineering, Sharif University of Technology, Tehran, Iran, in 2010, 2012, and 2017, respectively.

He was a Visiting Ph.D. Scholar with the Department of Energy Technology, Aalborg University, Aalborg, Denmark, from 2015 to 2016, where he is currently a Post-Doctoral Researcher. He was also a Visiting Researcher with intelligent electric power grids with the Delft University of Technology, Delft, The Netherlands, in 2019. His research interests include the reliability, control, and stability of power electronic-based power systems and renewable energies.

Frede Blaabjerg (Fellow, IEEE) received the Ph.D. degree in electrical engineering from Aalborg University, Aalborg, Denmark, in 1995.

He is honoris causa from University Politehnica Timisoara, Timisoara, Romania, and Tallinn Technical University, Tallinn, Estonia. He was with ABB-Scandia, Randers, Denmark, from 1987 to 1988, where he became an Assistant Professor in 1992, an Associate Professor in 1996, a Full Professor of power electronics and drives in 1998, and a Villum Investigator in 2017. He has authored or coauthored more than 600 journal articles in the fields of power electronics and its applications. He has coauthored four monographs and edited ten books in power electronics and its applications. His current research interests include power electronics and its applications in wind turbines, photovoltaic (PV) systems, reliability, harmonics, and adjustable speed drives.

Dr. Blaabjerg was a recipient of the 29 IEEE prize paper awards, the IEEE PELS Distinguished Service Award in 2009, the EPE-PEMC Council Award in 2010, the IEEE William E. Newell Power Electronics Award in 2014, and the Villum Kann Rasmussen Research Award in 2014. He was the Editor-in-Chief of the IEEE TRANSACTIONS ON POWER ELECTRONICS from 2006 to 2012. He has been a Distinguished Lecturer for the IEEE Power Electronics Society from 2005 to 2007 and the IEEE Industry Applications Society from 2010 to 2011 and from 2017 to 2018. In 2018, he was the President-Elect of the IEEE Power Electronics Society. He serves as the Vice-President for the Danish Academy of Technical Sciences. He was nominated by Thomson Reuters to be between the 250 most.

Peter Palensky (Senior Member, IEEE) received the M.Sc. degree in electrical engineering, the Ph.D. degree, and the Habilitation from the Vienna University of Technology, Vienna, Austria, in 1997, 2001, and 2015, respectively.

He has co-founded Envidatec, a German startup on energy management and analytics. He joined the Lawrence Berkeley National Laboratory, Berkeley, CA, USA, as a Researcher, and the University of Pretoria, Pretoria, South Africa, in 2008. In 2009, he became the appointed head of the business unit on sustainable building technologies at the Austrian Institute of Technology (AIT), Seibersdorf, Austria, and later the first Principle Scientist for complex energy systems at the AIT. In 2014, he was an appointed Full Professor for intelligent electric power grids at TU Delft, Delft, The Netherlands. His main research fields are energy automation networks, smart grids, and modeling intelligent energy systems.

Dr. Palensky is active in international committees such as ISO or CEN, and serves as an IEEE IES AdCom member-at-large in various functions for the IEEE. He is the Editor-in-Chief of the *IEEE Industrial Electronics Magazine*, an associate editor for several other IEEE publications, and regularly organizes IEEE conferences.